Journal of Medical Robotics Research, Vol. 0, No. 0 (2015) 1–15

Surgical Robot Platform With A Novel Concentric Joint For Minimally Invasive Procedures

Samir Morad[a], Christian Ulbricht[b], Paul Harkin[c], Justin Chan[c], Kim Parker[c], Ravi Vaidyanathan[c]

[a]*Department of Engineering, the University of East London, University Way, London, E16 2RD, UK*
E-mail: s.morad@uel.ac.uk

[b]*Charing Cross Hospital, Fulham Palace Road, London, W6 8RF, UK*

[c]*Imperial College London, Exhibition Road, SW7 2AZ, UK*

Abstract— In this paper, a surgical robot platform with a novel concentric connector joint (CCJ) is presented. The surgical robot is a parallel robot platform comprised of multiple struts, arranged in a geometrically stable array, connected at their end points via the CCJ. The CCJ joints have near-perfect concentricity of rotation around the node point, which enables the tension and compression forces of the struts to be resolved in a structurally-efficient manner. The preliminary feasibility tests, modelling, and simulations were introduced.

Keywords: surgical robotics, parallel robot platform, form-changing space frames, concentric connector joint.

1. Introduction

1.1. *Clinical Motivation*

Surgical robots have proliferated in recent years, with well-established benefits including: reduced patient trauma, shortened hospitalization, and improved diagnostic accuracy and therapeutic outcome. Despite these benefits, many challenges in their development remain, including how to improve instrument control and ergonomics whilst using rigid instrumentation with its associated fulcrum effects. Existing rigid instruments have restricted access to anatomical targets in-vivo and require well-planned incision points. Consequently, it is still extremely challenging to utilize such devices in cases that involve complex anatomical pathways such as the spinal column [1].

Malignant spinal tumors are cancerous and they spread and destroy the tissue surrounding them. Non-malignant spinal tumors can grow to a considerable size, causing damage by putting pressure on the tissue around them [2]. Surgical options for the treatment of spinal tumors vary from complete to partial removal. This may be done by a surgical approach from the front or back of the spine and may involve going through the neck, chest or abdomen. In critical cases, the surgeon may attempt to remove additional tumor growth by entering through the mouth or front part of the neck; however, this involves additional risk for the patient and is extremely challenging for the surgeon.

Currently, spinal surgical tools are reliant on drills and cutting tools which vary in their principles of operation. However, these tools cannot navigate around small corners present in the complex bones of the spinal column (Fig. 1-A). One of the most challenging procedures targets the removal of cancerous tumors sitting on top of and around the lumber vertebrae. At present, the surgeon approaches the patient from the back of the body, and the tumor is removed only from the posterior side of the spinal column using the available rigid tools, which are typically hand-held.

(A) (B)

Fig. 1. Non-reachable cancerous tissue (red) on the anterior side of the spinal column (A) [2], and photographs of the actual surgery taken as a part of this study (B).

This paper explores the mechanical design of a robotic framework, developed for use in this surgical procedure, as the guide and moving mount for an innovative surgical tool. The framework is a parallel manipulator, and uses novel concentric joints to simplify both the mechanical design of the framework and the kinematics. The design of a flexible surgical tool, capable of going around the spinal column for removal of tissue on both the anterior and posterior sides of the spinal column is briefly presented in [3] [4], and is intended to be introduced in detail in a separate paper.

1.2. *Parallel robots and spinal surgeries*

Surgery is one of the many fields of human endeavor where robots have been introduced due to their accuracy of

positioning, which exceed natural human capabilities. The evolution of surgical robots was achieved through a number of consecutive generations where many issues were improved from one generation to the next.

The configuration of most existing robotic surgery devices is based on the 'serial manipulator' configuration [3] [4], loosely analogous to the human arm—a series of struts (arms) with a hinged joint (elbow), along with pivots (wrist). An alternative configuration is the parallel manipulator configuration, where multiple struts form closed kinematic chains. The most common configuration is in the form of an octahedron, where two opposing rigid faces/plates are connected by six struts. These struts vary their length (telescope), and are connected via passive, free-rotation joints. This configuration is commonly known as a 'Stewart Platform' (or 'Gough-Stewart platform') [5] [6]. It has been adapted and used for several diverse applications, such as flight simulators [7], industrial process robots [8], and surgical platforms [9]. The term 'hexapod' is also used to mean an octahedral parallel manipulator.

Much work has been done comparing the two main robot configurations; in summary, serial manipulators have a larger working envelope in relation to their overall size [10], whereas parallel manipulators offer positional accuracy of the end effector, and smaller mobile mass than serial ones, thus allowing faster and more precise manipulations that are generally more suitable for medical applications.

Few parallel robotic systems have spinal applications, those that do have been developed for the positioning of pedicle screws [11]. Another system was developed for the replacement of cervical artificial discs [12]. However, the authors are not aware of any previous studies which have investigated or even mentioned the use of parallel robots for the resection of spinal tumors. In this paper a 6DoF parallel robot has been designed to guide and position a surgical tool for the resection of spinal tumor surrounding the spinal column.

To explain the evolution of the connector joint design used in the surgical robot parallel manipulator, the following section examines how the joint design originated from work on form-changing space frame structures, comprised of multiple telescopic struts.

1.3. *Space Frames*

Space frame structures emerged in the 1890s from work by A. G. Bell [13] related to structures for kites that were lightweight, but also strong. They are comprised from rigid struts joined together at their ends, configured as 3-dimensional trusses. Figure 2-A, B shows examples based on struts in square pyramidal/tetrahedral and octahedral/tetrahedral arrangements. Historically, these frames have used struts of fixed lengths to create rigid structures.

Figure 2-C shows a close-up view of a rigid space frame, comprised of fixed-length struts (S). The angular displacement (AS) between all the struts does not change; therefore, the struts can be connected at the vertices (or nodes) via simple rigid joints at the convergence points (CP), which are often spherical in form (J_S).

Figure 3 shows a simplified, detailed view of the same fixed spherical joint (J_S). It is important that the struts' axes, and therefore the lines of force (LF) all need to intersect at CP at the nodes. This alignment, along with the use of triangulation in 3

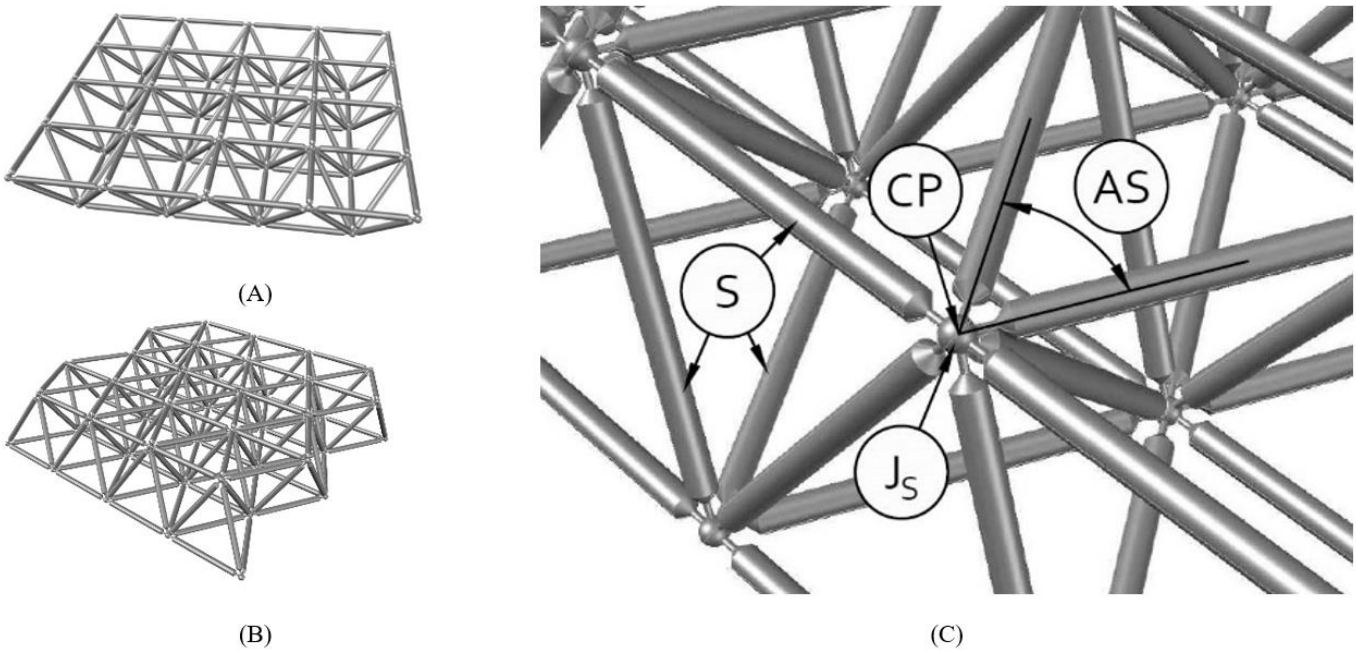

Fig. 2. Space frames – (A) pyramidal/tetrahedral, (B) tetrahedral/octahedral arrangements, (C) Space frame node with rigid joint

dimensions, means loads imposed upon the structure are resisted almost wholly via tension forces (F_T) or compression forces (F_C) along the axes of the struts forming the frame, with little or no shear or bending forces acting upon the struts [14]. Thus, the struts only have to resist elongation from tension, or buckling due to compression. This leads to a very efficient structure for a given quantity of material, i.e. they have excellent strength-to-weight ratios.

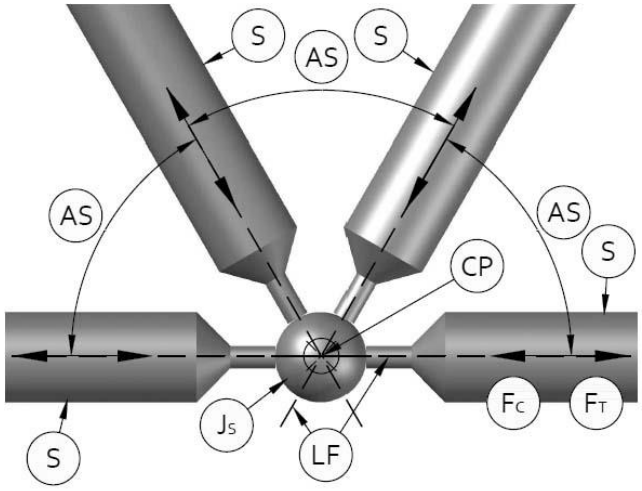

Fig. 3. Space frame node – rigid joint detail

It will be seen that there are at least 3 struts converging at any of the nodes within a space frame, and this can increase to 8 in a pyramidal/tetrahedral arrangement of the frame, or 9 struts in the tetrahedral/octahedral frame, both shown in Figure 2-A and 2-B. If the frame is double-layered, up to 12 struts converge at the nodes for either arrangement.

1.4. *Form-Changing Space Frames*

A distinctive type of form-changing space frame structure has emerged in engineering design since the 1940s; these can act as both a rigid structure in a variety of fixed forms, or continuously vary their form, depending on the requirements of a wide variety of applications. They are linear actuators that have struts that can change their length (or 'telescope') in a controlled manner, connected together pivotally at their ends, and arranged in the same geometrically-stable forms as rigid space frames. By varying the length of the struts, the frame can assume a wide variety of forms.

A widely-used version of this type of structure is the Gough/Stewart Platform [5]. Since the 1990s, there has been growing interest in frames comprised entirely of telescopic struts, with no rigid sections, which are inherently able to assume a wide variety of forms. The near-concentric node joints examined in this paper were originally developed for this type of form-changing space frame. However, this paper focuses on the parallel hexapod manipulator configuration featuring rigid upper and lower plates, where the use of near-concentric node joints still offers intrinsic advantages [15].

2. The Design of the Concentric Joint

2.1. *Requirements for the joint*

In a form-changing space frame, the struts can change length independently of one another. Therefore, at each node point, a joint is required where at least 3 struts need to pivot with 3 degrees of freedom (3DoF) around the nodes where the ends of the struts are connected. The pivot point needs to be at the node point of the space frame to ensure the struts form the triangles that are key to the frame's stability and structural efficiency so the pivot points must be concentric. In both nature and man-made objects, there are countless joint mechanisms that connect together 2 elements that can pivot around a point with 3DoF, e.g. the ball-and-socket joint found in the human shoulder. Joints that enable this for 3 or more convergent struts are not thought to exist in nature, at least not with a close degree of concentricity of the pivot points, so inspiration cannot be sought from there. Neither do they appear to have been developed beyond the prototype stage in the field of mechanical engineering.

2.2. *Inherent weaknesses of ball-and-socket joints*

On first examining the problem, the authors first considered using multiple ball-and-socket joints, clustered together at the nodes. Figure 4-A shows a joint assembly of 3DoF ball-and-socket joints (J_{BS}). The non-concentric pivot points (PP) of the joints are separated by distance D. The separation is necessary as this mechanism is not able to be transposed into the same volume as another. F_C and F_T acting along the axes of the struts are shown as LF. With the angles of separation (AS) between the struts as shown, the lines of force intersect at a convergence point (CP) of the central connection (CC), and the struts are not subject to shear or moment forces.

Figure 4-B shows the same joint arrangement, but with forces of compression (F_C) acting upon the struts (S). CC component has been made to rotate due to the loads from the struts acting as moment forces (F_M) upon it. LF now do not pass through the convergence point (CP). At the ball-and-socket joint J_{BS1} the strut (S_1) connected to the ball is now in contact with the socket edge of the socket at point P_1. Thus, a load resulting in a F_C upon strut S_1 would impose a bending moment at this point of contact (P_1) upon the end of strut S_1 as it induces further rotation of the central connection. The intrinsic structural efficiency of the space frame structure is compromised, as its struts now have to resist shear and bending forces, rather than simply F_T and F_C loads along their primary axes.

Should the loads on the struts (S) change to F_T (blue arrow), the central connection will rotate back in the opposite direction (blue rotated arrow), as the struts exert a pulling force upon it via the ball/socket joints. This rotation could be sudden, and difficult for any control system to predict. This rotation amounts to localized instability of the joint assembly. For the overall framework, the accumulation of these localized instabilities

would lead to wider patterns of more pronounced and uncontrolled instability.

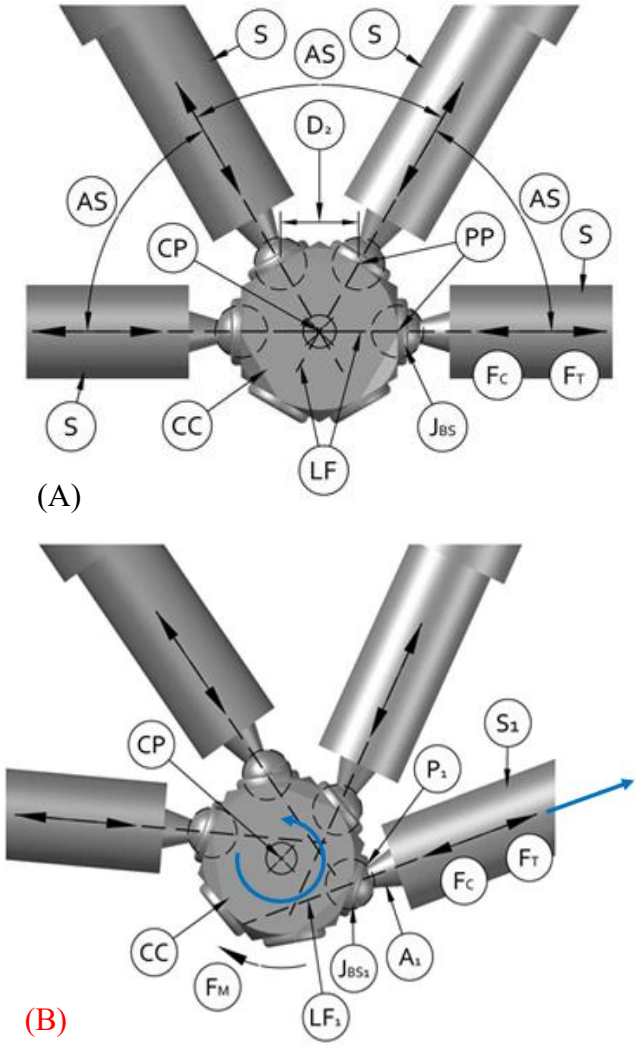

Fig. 4. Ball and socket joints – (A) aligned, and (B) misaligned

2.3. *Mechanisms for concentric joints*

Most hexapod robots are not truly octahedral in their form, due to the layout of the joints at their vertices. The connections between the struts and the rigid plates are via joints with 2DoF, in the form of revolute/hinge joints. Typically, however, these joints are configured so that each strut has a separate connection to one of the rigid plates (Fig.5A), rather than being concentric with the end of the adjacent strut (Fig.5B). Rather than a pure octahedron, it will be seen that this forms a more complex geometric shape comprised of a pair of irregular hexagons (the rigid plates), connected via the variable-length struts, pairs of which form 'skew quadrilaterals.' In geometric terms, the whole form is a 'skew hexagonal prism.'

In order to create a geometric structure that is much closer in pure geometry to an octahedron, with all of the benefits of simplicity this would bring, it will be seen that the commonly-used 2DoF pin joints need to be replaced with a different joint configuration. The preferred joint type would allow adjacent pairs of telescopic struts to share a common connection point with the rigid plates (thus three components are connected), and this same point would act as a center of rotation for the end points of the struts.

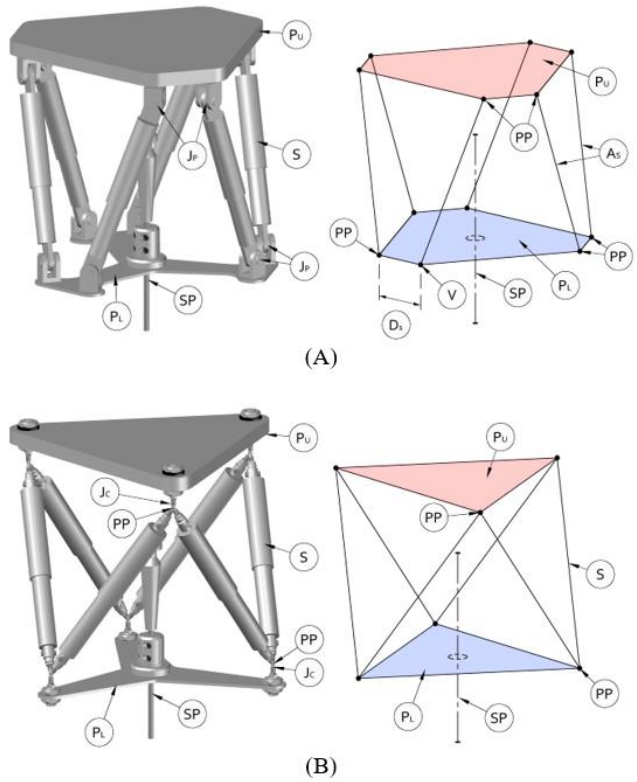

Fig. 5. (A) Non-concentric joints are configured so that each strut has a separate connection to one of the rigid plates, (B) Concentric joints allow the struts to be concentrically connected to each other and the rigid plates.

As part of the growing interest in variable geometry truss structures within the robotic community since the 1990s, several research groups have been developing novel designs for truly concentric free-rotation joints (Fig. 6), such as those by [16,17].

What initially appears to be a simple requirement (design a mechanical joint allowing more than two linked struts/links to share a common center of rotation) turns out to be a deceptively difficult task to solve. This may be due to the relatively rare instances where such a joint would be required. Virtually all mechanical joints with more than 1DoF connect only a pair links. In those applications where more than two components are intended to be joined together, such as a hexapod

manipulator, it is typical for multiple copies of distinct two-link joints to be grouped together as closely as is practical. This compromise is adequate in a mechanical sense for many purposes, but then concentricity is clearly not achieved. For the kinematics that control such a device, measures must be taken to work around this non-concentricity, e.g. the use of more complicated formulae to calculate the geometric form of the device.

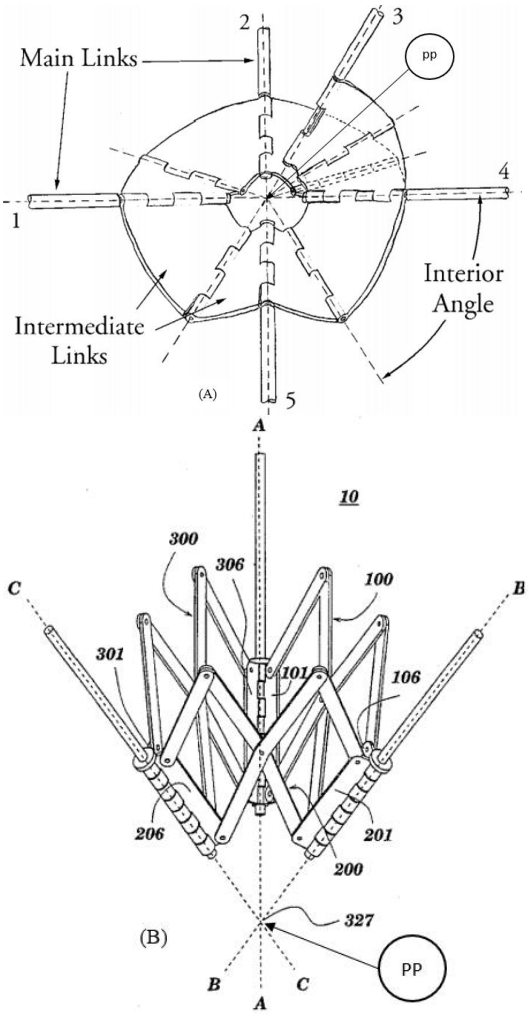

Fig.6. Concentric joints by (A) Bosscher/Ebert-Uphoff, and (b) Hamlin

To simplify the kinematics, the joint configuration proposed by both Bosscher/Ebert-Uphoff and Hamlin allow more than two moving components to be pivotally connected with concentricity. Thus, they seem to solve the problem of a joint at the node points of a parallel robotic framework. However, both examples in [16] and [17] use relatively bulky and complex mechanisms, with many moving parts. Instead, a concentric joint design was sought that was simple, compact, robust, and used few, if any, moving parts.

To still achieve the same mechanical goals, but offering a simpler, more compact joint configuration, the novel Concentric Connector Joint was used in the design of the surgical robotic framework, originally developed by the authors for use in prototypes of form-changing space frame structures [15][18].

3. Path Towards A Solution

3.1. *Tension structures*

For the resolution of purely tension loads, multi-link concentric joints that can resolve tension forces, but not compression, have been in common use for millennia—one example being those within a structure woven from flexible fibers or cords, such as a fishing net.

However, for the many potential applications where a form-changing space frame structure might be used, both tension and compression forces occur within the struts. Hence both types of loads must be resolved by the nodal connections.

3.2. *Resolving tension and compression forces*

A way was sought to utilize the simplicity and efficiency of a tension-based network comprised entirely of flexible cords, yet also have it resist compressive forces. The key insight was to re-examine the joints within rigid space frame structures, and understand how these resisted compressive forces, and then see if the principles could be combined with the efficiency and simplicity of the tension cords.

For the example shown in Figure 2-C, the frame's struts join together at their ends via their connection to solid blocks, which are typically spherical in form. For commercially-available rigid space frames, the spheres act as a convenient method of joining the struts together, thus extending the material structure of each strut towards the node point, where the tension/compression forces are transmitted to the conjoining struts. Instead of the sphere, the struts themselves could be extended as close as practical to the node point, and joined directly to the other adjoining struts, such as by welding or bonding (i.e. gluing). As the struts are subject to compressive forces along their lengths, the ends at the joints have a tendency to push onto the adjacent strut end. In effect, the strut is attempting to push through and then past the ends of the other struts.

3.3. *Use of cords to tie struts together*

But what if the joining by bonding of the strut ends could be done via the flexible cords of the net structure, passing through the ends of the struts, and entwining with other cords from other struts, thus tying the ends together? A compressive load, pushing along the axis of the strut, would, as above, be induced to push the end of the strut through and then past the ends of the other struts, but the cord would prevent it from doing so. When the strut is subject to a tension force, the cord would resist this by itself going into tension. Due to the ends of the struts not being joined rigidly to each other, but only pulled into contact

with each other by the flexible cord, they can effectively pivot relative to each other, giving 3DoF. Figure 7 shows a cross-section view through the joint configuration. This shows the ends of the struts (S) as tubular forms, with collars (CL) inserted in their ends, which in turn have lengths of cords (C) passing through them. The cords are knotted at their ends (KN) to prevent them passing through the collars, and are entwined with other cords to retain the strut ends.

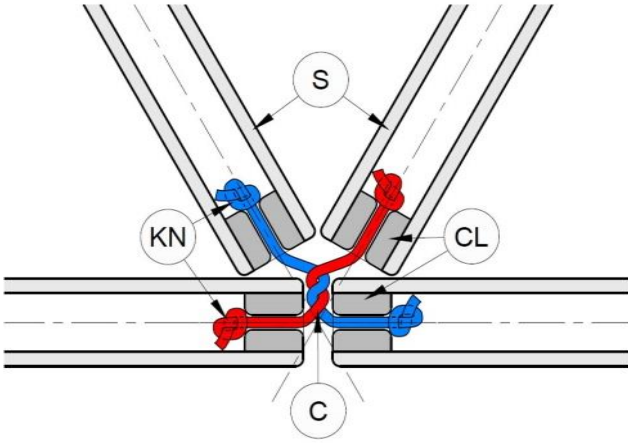

Fig. 7. Cross-section of struts tied together with cords

3.4. *Refinements to the design*

This crude arrangement would function as a 3DoF joint for 3 or more struts, but there are some important refinements that can be made to greatly improve the joint's performance, shown in Figure 8-A and 8-B.

As the tips of the struts are in moving contact with one another, the extremities of struts have been formed as relatively short tubular barrels of a low-friction bearing material (B_N). Nylon 66 (a type of polyamide) was chosen in prototypes due to its balance between reasonable resistance to bending forces, low friction properties and good resistance to impact loading; it was accepted that relatively minor deformations of the nylon tips would add to the joint's overall robustness, with only a negligible effect on the joint's overall concentricity within the frame. The cord passes through the barrel, emerging to entwine with other cords. A relatively non-brittle material such as nylon is also suitable as it directly contacts the cord and exerts a pressure upon it, e.g. when the strut is subject to a compressive force, it attempts to push past the other barrels and shear the cord.

A 2-piece end collar (CL_1, CL_2) with a conical form is located at the end of each strut (S); so their cross-sectional area decreases towards the node point. This provides rigid support for the barrel and in turn the cord very near to the convergence point at the node. This partially overcomes the issue noted previously; the seemingly conflicting desire to locate rigid materials as close as practically possible to the point where the struts join together, whilst still allowing clearance for the struts to pivot around the node point.

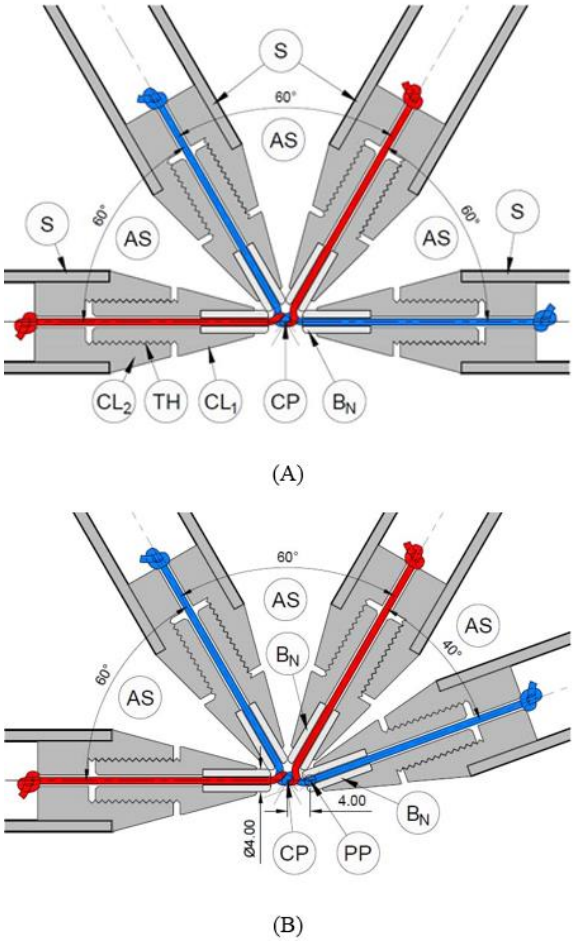

Fig. 8. Cross-section of tapering cord joint. (A) aliened strut, (B) pivoting strut.

3.5. *Cord tension adjustment and elasticity*

Collars CL_1 and CL_2 are threaded together; their rotation relative to each other varies the distance between KN and the barrel (B_N), thus giving a convenient method of adjusting the tension in the cords.

It is an important factor for the cords to have a slight degree of elasticity whilst the struts pivot around the node point, their length would need to vary slightly depending on the angular displacement of the struts. The degree of this elasticity would have to be chosen carefully, as it would need to balance sufficient 'slackness' to allow the struts to pivot freely versus ensuring the strut ends maintain contact with one another. The elasticity would also have to be chosen to resist the tensile/compressive forces imposed by the struts on the joint.

3.6. *Concentricity*

It is acknowledged that the proposed joint design has less than perfect concentricity of the pivot points of the struts. Figure 8-B shows that the actual PP is not at the original convergence point (CP), but closer to the rounded contact point between the barrels (B_N) at the ends of the struts. In the built prototypes, the distance between the node point and the actual pivot point was approximately 4mm. This displacement of concentricity appears to be proportional and approximately equal to the diameter of the barrels (4mm). This displacement distance is smaller than could practically be achieved using multiple ball-and-socket joints. It is also proportionally low relative to the overall length of the telescopic struts of the prototypes (which vary in length from 450mm to 270mm); the displacement of concentricity is between 0.9% and 1.5% of the strut length.

4. Analysis of the Design of the Surgical Robot Platform

4.1. *Overview*

According to the surgical requirements set by our collaborator surgeon, it is necessary that the surgical cutting tool (T) be positioned and moved around the dorsal parts (e.g. the vertebral cavity VC) of patient (P), who would be lying face-down during the surgical procedure (Fig. 9). A parallel manipulator robotic platform has been designed that acts as a mount for the tools (T), and produces the desired range of movements.

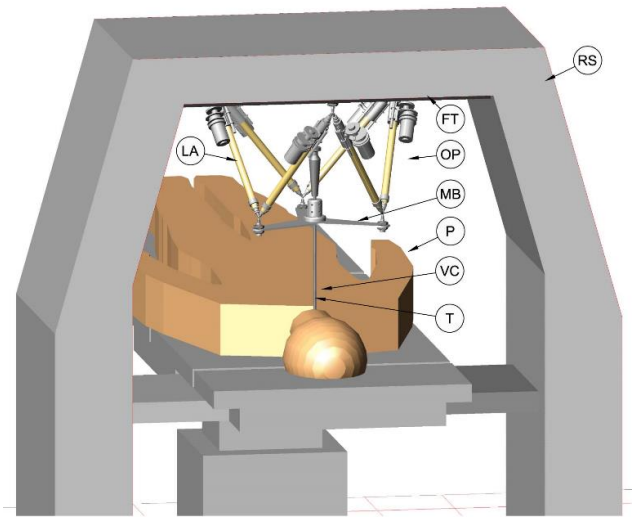

Fig. 9. An illustration of the assembled surgical robot device installed in an operating theatre environment. (T) Surgical tool, (VC) vertebral cavity, (FT) fixed top, (LA) linear actuators, (MB) mobile base, (P) patient, (OP) octahedral platform, and (RS) rigid structure.

The octahedral platform is 6DoF parallel manipulator, which is comprised of a fixed top (FT), and a mobile base (MB), connected by six individually-powered extensible linear actuators (LA) or legs. The octahedral platform is intended to be suspended from a rigid structure (RS) located above the prone patient (P).

4.2. *Configuration of the surgical platform*

The robot manipulator was designed such that it will be suspended from a fixed structure located above the patient. This requirement is a consequence of the prone, facedown posture of the patient during the surgical procedure. The structure of the suspension system simply has to provide three rigid attachment points for the topmost triangular face of the octahedral robotic framework.

The aforementioned practical limits on the range-of-movement for the robotic framework (an approximate sphere (S) of 120mm diameter), and the consequence of having to reposition the support structure to enable access to as much of the length of the vertebral cavity as possible (700mm in length), result in the need to consider how the support structure itself is configured/fits around the patient (Figure 9).

There are two possible configurations of the surgical platform:

(i) Mounted from a fixed structure above the surgical table (e.g. suspended from the ceiling of the operating theatre), possibly in the form of rails that run parallel to the patient's spine, to allow the robotic framework to move along them.

(ii) An independent floor-bearing structure that straddles the operating table. This could be achieved by using a trolley in the form of an inverted U-form, that could fix to the table, and then move relative to it as needed along the length of the patient's spine. In other words, making RS moving along the length of the patient's spine.

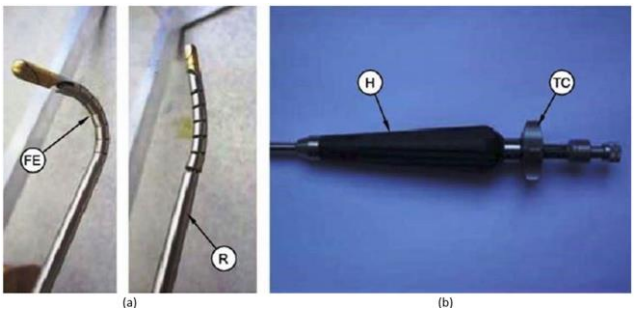

Fig. 10. The flexion unit. (a) A retractable lower distal tip fully tensioned and fully released. (b) Proximal end with the attachment of tensioning screw.

4.3. *The Articulated Distal Tip Tool*

An Articulated Distal Tip (ADT) tool was constructed [19] to the design specifications according to the angulation principles (Fig.10). The tool is a surgical Retraction Instrument with an

adjustable articulated tip (FE), and an overall length of approximately 250mm. It is primarily formed from a 5mm diameter hollow round shaft (R) of SAE grade 304) steel—18% chromium and 8% nickel. A handle (H) near the proximal end is formed from polyphenylsulfone (PPSU) plastic material. A revolving nut/tensioning screw (TC) is located beyond the handle at the proximal end.

The FE is comprised of steel, with the cables routed within the R. When the cables are tightened, via a threaded mechanism connected to the TC, the tip bends to form an approximate arc or J-shape, with the radius of the arc diminishing as the tension increases. Conversely, as the cable tension decreases, the adjustable tip resumes its default near-linear form. Thus, the tip can be bend in a controlled manner up to approximately 120° from the shaft axis.

4.4. *Range of Movement and Working Envelope*

The vertebral cavity (VC) containing the spinal column (Fig. 11) of a typical prone adult patient (P) has a cross-sectional area of very approximately 60mm width and 80mm height, and an average length of approximately 700mm.

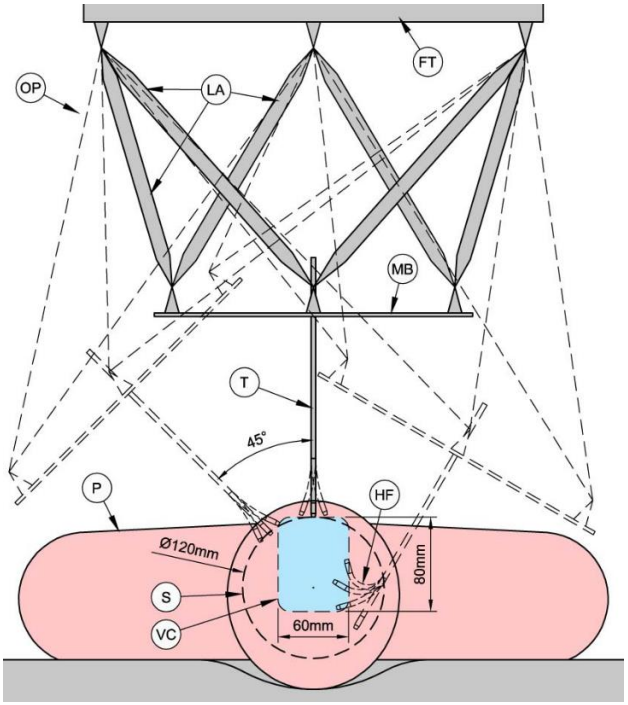

Fig. 11. Surgical tool (T) working envelope relative to vertebral cavity (VC). (FT) fixed top, (LA) linear actuators, (MB) mobile base, (HF) hook-like form, (P) patient, (S) approximate sphere, and (OP) octahedral platform.

However, with reference to Fig. 1, it will be seen that the tumors that are the device's target are typically less than approximately 100mm in length along the axis of the spinal column. Therefore, it was decided that the surgical cutting tool (T) needs to access a section of the vertebral cavity only approximately 120mm in length, rather than the full 700mm of the spinal column. This helped to simplify the mechanism, and prioritized end effector accuracy within a smaller working envelope.

Taking the spinal column as being very approximately cylindrical in form, and based on the dimensions as above, the end-effector working envelope was established as an approximate sphere (S) of 120mm diameter. Based on the ability of ADT tool to assume a hook-like form (HF) around the spinal column, the platform was configured to give an angular displacement of ±45° from the z-axis, thus giving the surgical tool complete access to all sides of the spinal column.

5. Robot Platform: Detailed Design

Based on the above-mentioned octahedral configuration, and to create a device that was considerably lower-cost than those that are commercially available, a simplified design of the platform was developed for the moveable mounting platform for the surgical tool.

5.1. *Linear actuator*

For the variable-length linear actuators, or legs, a relatively simple single-portion extension configuration was used. This configuration was preferred over multiple-portion extension devices; these are normally used when the retraction/extension ratio needs to be greater than 1:1.7. Typical applications for multiple-portion extension devices are for long-span crane booms that must be relatively compact when transported, or retractable radio aerials. For any given method of powered extension/retraction, their design tends to be more complex than for single-portion actuators.

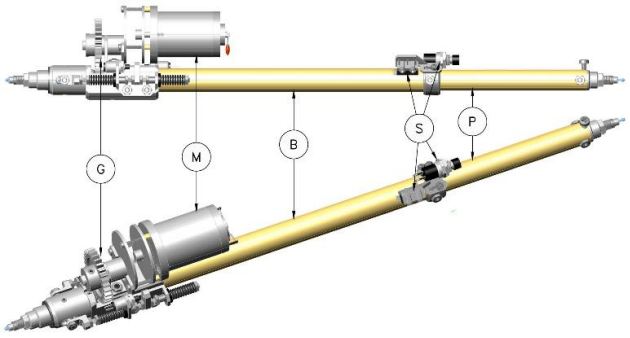

Fig. 12. Variable length linear actuator. (P) Piston, (B) barrel, (M) motor, (G) gear, and (S) switch.

With reference to Fig. 12, the single-portion actuator comprises only two main groups of components: an outer, cylindrical 'barrel' (B) and a corresponding inner 'piston' (P). The ratio of the fully-retracted/fully-extended length of the whole assembly should be 1:2. However, this is only a theoretical ratio, as it is usually a slightly lower ratio (typically

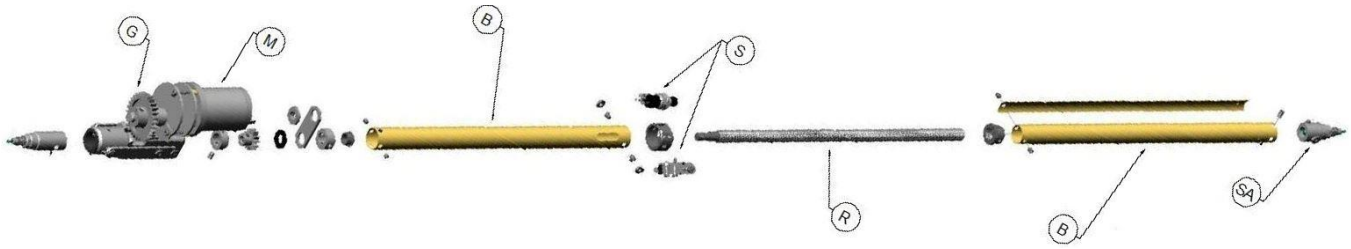

Fig. 13. An isometric view of an expanded plot of the linear actuator: (G) gear, (M) motor, (B) barrel, (S) switches, (R) rod, and (SA) sub-assemblies.

1: 1.7). Typically this is due to there being portions of the overall length of the actuator that do not fully retract into the barrel (e.g. seals/collars, or fixed-length connecting joints), and the need to prevent the piston from fully emerging out of the cylinder, as there must always be a certain overlap of the lengths of the two components at the point of maximum extension.

The 'stroke' of a linear actuator is the variation in length of the whole assembly as it goes from maximum retraction to maximum extension, whilst accounting for any portions of the design that are either fixed in length/do not fully retract, and/or any overlap at maximum extension.

In the prototype, the lengths when fully retracted/ fully extended are approximately 270mm and 450mm respectively—a ratio of approximately 1:1.7. A single lead screw mechanism, powered by a DC motor (M) via a gear assembly (G), produces the linear movement.

For the main lengths of the actuator portions that extend/retract, brass was chosen as it has a relatively low tendency to 'gall' when used in sliding contact with other metals. In addition, the ions in copper alloys, such as brass, are both antiviral and antibacterial. Collars that act as interfaces/bearing between the brass portions, and revolute bearings were fabricated in stainless steel (SAE grade 304), due to it being a reasonably hardwearing material and having good bearing properties. The 'nuts' of the leadscrew mechanism were originally fabricated in stainless steel, but these had a tendency to jam the leadscrew mechanism, due to even quite minor manufacturing misalignments. They were therefore refabricated in nylon 6 (Polycaprolactam), a material commonly used in mechanical bearing applications, which overcame the jamming problem.

For other, non-moving components, such as various brackets and the main mounting block, which connects the motor/gearbox assembly to the brass actuator portions, aluminum was chosen for its easy machining properties and low relative weight.

5.2. *Prismatic bearings*

For mechanisms where a lead screw is used, it is necessary to incorporate measures to prevent rotation of the various portions of the actuator relative to each other along the axis of the lead screw. Otherwise, there might be tendency for the rotation of the lead screw to simply rotate the portion intended to be extended/retracted, due to friction between the lead screw and the internal thread. This can be avoided by using a 'key' in either the barrel or piston, which engage/slides within a 'keyway' or slot within the other portion. This permits the actuator portions to move relative to each other along their shared principal axis, but not rotate around it, in other words, it acts as a 'prismatic' bearing or joint. Figure 13 shows an expanded engineering drawing of a complete 'leg' with all sub-components.

5.3. *Modified connector joint*

To connect the linear actuators/legs to the stationary/fixed top and lower mobile base, near-concentric connector cord joints (Figure 14-A, B), were developed and manufactured for the prototype, based on the principles described in section 3. These were originally developed for use in variable-geometry space frames (Figure 14-C, D).

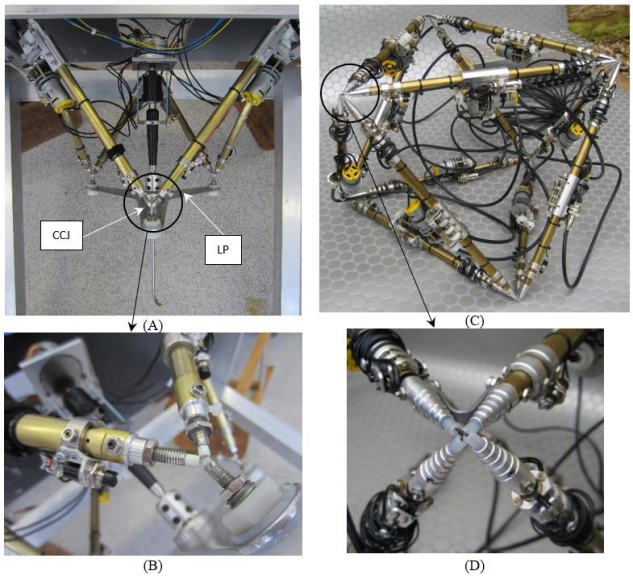

Fig. 14. A concentric connector joint as part a prototype surgical platform (A, B) and Tapering Cord Joints as part of a prototype octahedral-frame (C, D).

The joints (Fig. 15) consist of a number of sub-assemblies (SA), which each connect to the ends of the LA and the mobile base (MB). A flexible, slightly elastic cord (C) passes through each subassembly. The cord is precisely adjusted via a threaded mechanism (TM) to pre-tension it. The tips of the sub-assemblies are hollow barrel forms (HB), through which the cord passes, and the ends of the cords are tightly intertwined with each other. The pre-tensioning of the cord pulls the ends of the nylon barrels together, thus allowing free rotational movement, but resisting the primarily tensile and compressive forces imposed by the legs.

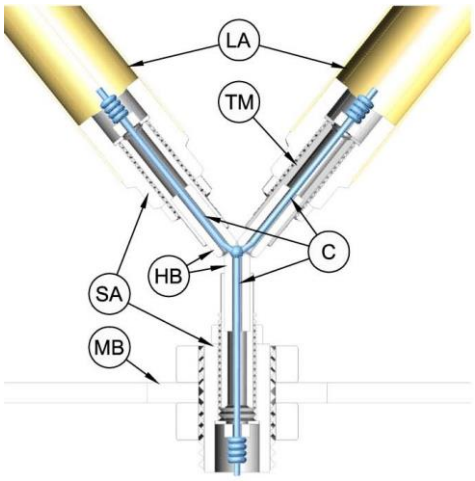

(A)

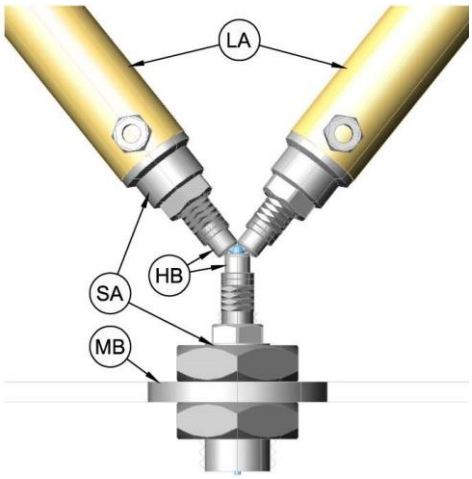

(B)

Fig. 15. Connector joint assemblies, shown in (A) section and (B) side view. (SA) sub-assemblies, (LA) linear actuators, (MB) mobile base, (C) elastic cord, (TM) threaded mechanism, and (HB) hollow barrel.

5.4. *Other design considerations*

Switches (S) were incorporated into the design of the linear actuators (Fig. 12), which act as motor cut-out devices at the point of maximum extension or retraction, primarily to prevent the drive mechanism from breaking components when the mechanical limits of the actuator stroke are reached.
Rotary encoders are installed on the motor/gearbox shaft, as a means of measuring the revolutions of the motor, and hence calculate the extension/retraction of each actuator.

The form of the platform's lower plate (LP) has been determined by the need to make it as rigid as possible, whilst at the same time minimizing the visual obstruction it creates for the operator/surgeon (Fig. 14).

6. Kinematics of the Robot Platform

It is necessary to calculate the required leg lengths of each of the six platform legs in order for the robot platform to control the desired orientation of its end-effector as specified by the user. Based on [20, 21], the inverse kinematic was formulated for the 3-3 parallel octahedral platform.

What follows will be a brief description of the Euler's equations used to solve this system. For convenience, the important notations used here are presented in Table 1.

Table 1. Description of the notations used in the calculation of the inverse kinematics.

Symbol	Physical description
φ	Rotation about X-axis
θ	Rotation about Y-axis
Ψ	Rotation about Z-axis
R	Rotational matrix
P_i	Attachment point of leg ***i*** in the top plate
P	Position of the top plate relative to the base plate
B_i	Attachment point of leg ***i*** in the base plate
L_i	Nominal length of leg ***i***

The configuration of a 3-3 robot platform can be seen in Figure 16. There is a total of six pairs of concentric spherical joints; three on the top B_1=B_6, B_2=B_3, and B_4=B_5 and three on the end effector P_1=P_2, P_3=P_4 and P_5=P_6.

In order to progress further into the analysis, it is important to define two separate coordinate systems; the fixed Cartesian coordinate system X, Y and Z which are attached to the base and has its origin at the center of the base, and the end-effector coordinates system x, y and z attached to the end-effector with its origin located at the geometric center of the top plate.

The position of the end-effector is denoted by P and given by the expression:

$$P = [x \quad y \quad z]^T \tag{1}$$

It follows from the kinematics of each leg that the closed loop position vector equations are given by:

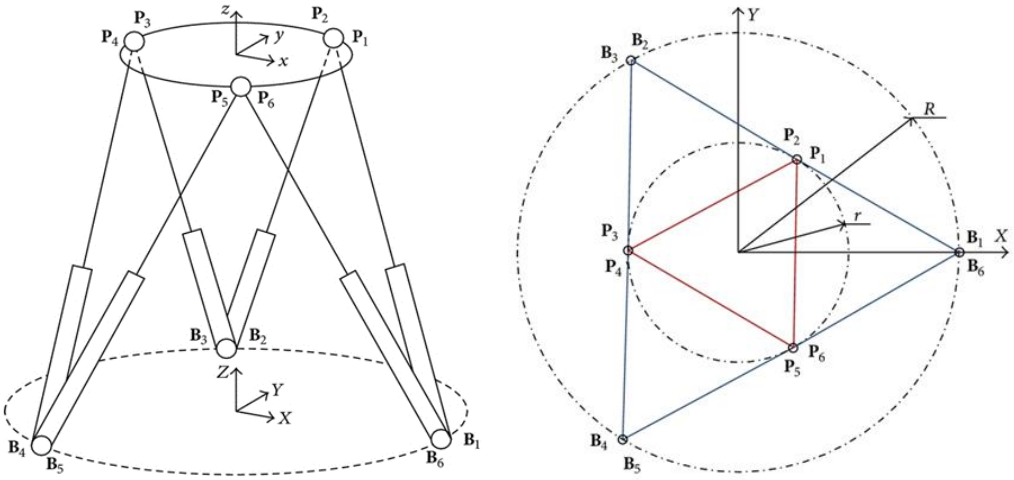

Fig.16: The configuration of a 3-3 robot platform. (A) Isometric view and (B) plan view show the attachment points of the six links to the fixed top (B) and to the moving platform (P).

$$R = R_Z(\Psi)R_Y(\theta)R_X(\varphi)$$

$$R = \begin{bmatrix} \cos\Psi & -sin\Psi & 0 \\ sin\Psi & cos\Psi & 0 \\ 0 & 0 & 1 \end{bmatrix} \begin{bmatrix} cos\theta & 0 & sin\theta \\ 0 & 1 & 0 \\ -sin\theta & 0 & cos\theta \end{bmatrix} \begin{bmatrix} 1 & 0 & 0 \\ 0 & cos\varphi & -sin\varphi \\ 0 & sin\varphi & cos\varphi \end{bmatrix}$$

$$R = \begin{bmatrix} cos\Psi cos\theta & -sin\Psi cos\varphi + cos\Psi sin\theta sin\varphi & sin\Psi sin\varphi + cos\Psi sin\theta cos\varphi \\ sin\Psi cos\theta & cos\Psi cos\varphi + sin\Psi sin\theta sin\varphi & -cos\Psi sin\varphi + sin\Psi sin\theta cos\varphi \\ -sin\theta & cos\theta sin\varphi & cos\theta cos\varphi \end{bmatrix} \quad (2)$$

$$L_i = \begin{vmatrix} L_{ix} \\ L_{iy} \\ L_{iz} \end{vmatrix} = \|RP_i + P - B_i\| \quad (3)$$

Where P_i and B_i are given by the expressions:

$$P_i = \begin{bmatrix} P_{ix} \\ P_{iy} \\ P_{iz} \end{bmatrix} = \begin{bmatrix} r_p \cos(\lambda_i) \\ r_p \sin(\lambda_i) \\ 0 \end{bmatrix} \quad (4)$$

$$B_i = \begin{bmatrix} B_{ix} \\ B_{iy} \\ B_{iz} \end{bmatrix} = \begin{bmatrix} r_B \cos(\Lambda_i) \\ r_B \cos(\Lambda_i) \\ 0 \end{bmatrix} \quad (5)$$

Where r_P and r_B are the radiuses of the points to the centre and λ_i and Λ_i are:

$$\lambda_i = \frac{(i-1)\pi}{3}, \qquad \Lambda_i = \frac{i\pi}{3}; \qquad \text{for } i = 1,3,5 \quad (6)$$

$$\lambda_i = \lambda_{i-1} + \frac{2\pi}{3}, \qquad \Lambda_i = \Lambda_{i-1}; \qquad \text{for } i = 2,4,6 \quad (7)$$

Solving Equation 3 using Equations 1, 2, 4, 5, 6 and 7 gives the nominal lengths for all six legs of the robot platform for any given input of x, y, z, φ, θ, and Ψ.

7. Simulation Results

The design of the surgical platform was based on the classic Stewart platform for positioning objects. The platform has an exceptional range of motion and can be accurately and easily positioned and oriented. The platform provides a large amount of rigidity, or stiffness, for a given structural mass, and thus provides significant positional certainty. In this section, the behavior of the platform is demonstrated using Simulink, with SimMechanics to model the mechanical components of the system. Figure 17 shows the complete platform model.

The preliminary validation of the design of the platform was performed by simulating the model system. The output data on the behaviour of the platform system was obtained graphically and numerically and displayed in the MATLAB workspace via a position sensor block. This block contains sensors that sense the position of the X, Y, and Z coordinates of the end effector.

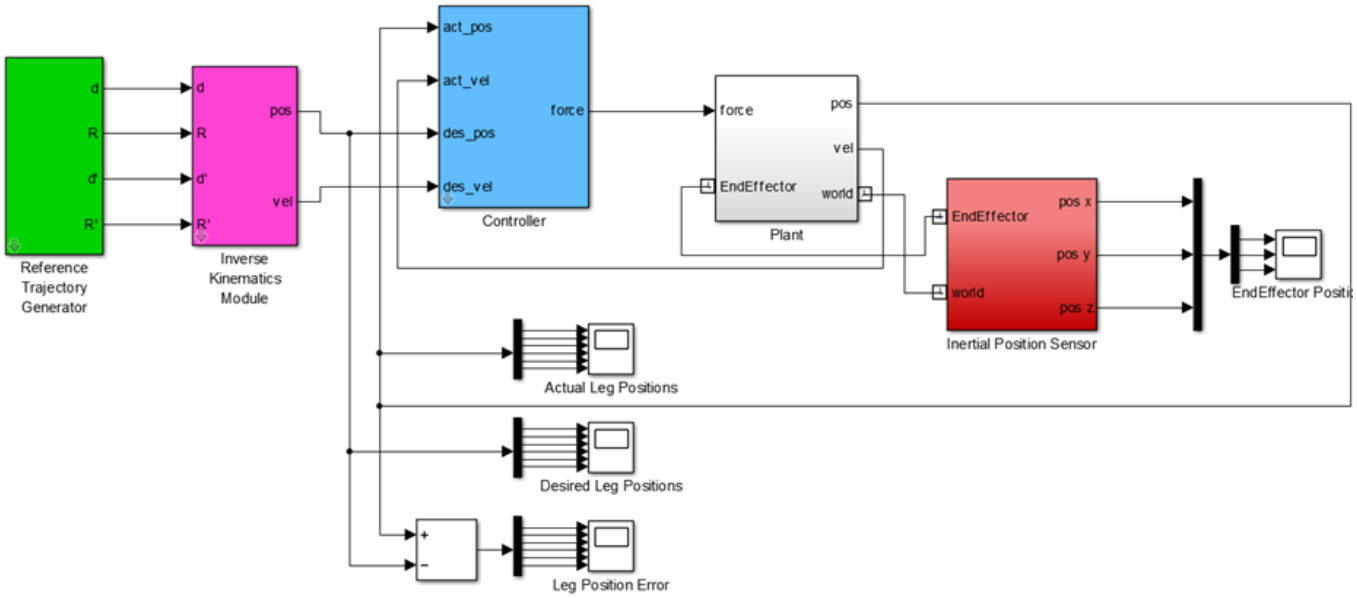

Fig.17: The complete surgical platform model. The physical plant is connected to the controller model, which is encompassed of inverse kinematics and trajectory models, to perform simulation. The model is also connected to several displays representing positioning data.

Figure 18-A shows the x, y, and z values of the position of the body block representing the end effector moving over time as the model simulates. The numerical data of the end effector position (X, Y, and Z) was used to plot a 2-D/3-D representation of the end effector path (Figure 18-B) and volume (Figure 18-C).

8. Discussion

The concentric connector joint, originally developed for use in variable-geometry space frames, was modified and used in the development of a parallel robot platform for this medical application.

Because of the 'powered' nature of our flexible surgical tool (to be introduced in a separate paper), by means of either mechanical drill or a fluid high-pressure pump, the handheld use of the tool is prone to vibration and fluid impact force. Consequently, this leads to control difficulties during critical operation procedures. Hence, implementing a robot was vital to ensure the surgical task was performed safely by increasing the stability, and therefore the accuracy of the tool, especially as it was moving.

Within the different robot structures, there are also advantages and disadvantages that determine the suitability of a certain robot structure for a particular task. The high accuracy and stability of a parallel robot performing in a small workspace led to it being designed, manufactured, and integrated into our flexible surgical device, as it is the most suitable robot for our surgical application.

For the parallel robot mobile platform, aspects of the earlier configuration of a form-changing space frame were adapted and simplified, to create a parallel platform with a fixed top and mobile base, connected via six extendable legs. The re-designing process has simplified the structure so it would be more appropriate for use in an operating theatre and can be controlled remotely.

For the concentric connector joint, it is possible that the joint would ultimately fail due to compression loading once the cord elongated to such a degree that the tip of one strut passed beyond that of the others, leading to two eventualities. One is that the cord would be elongated beyond its elastic limit and its elongation becomes irreversible (or plastic), then when the compressive load is removed, the strut end would no longer be in contact with the adjacent strut ends, leading to loss of concentricity. The second is that the 'barrel' tubular form at the end of the strut would be subject to a concentrated bending moment as the cord would still be restrained by the other struts, likely leading to its permanent deformation and/or disintegration.

Failure due to tension loading would occur when the cord elongates beyond its elastic limit; when the load was removed, this would lead to a similar lack of contact between the strut ends as above.

Obviously, in addition to the cord elongating beyond its elastic limit in either scenario noted above, the ultimate failure of the joint would occur should the cord break. In the prototype joints, the cord chosen ('Beta Saltwater Mono 80lb Clear' by Shakespeare Fishing) was a monofilament fishing line of 1.2mm diameter, with a breaking load of 36kg, which also has a

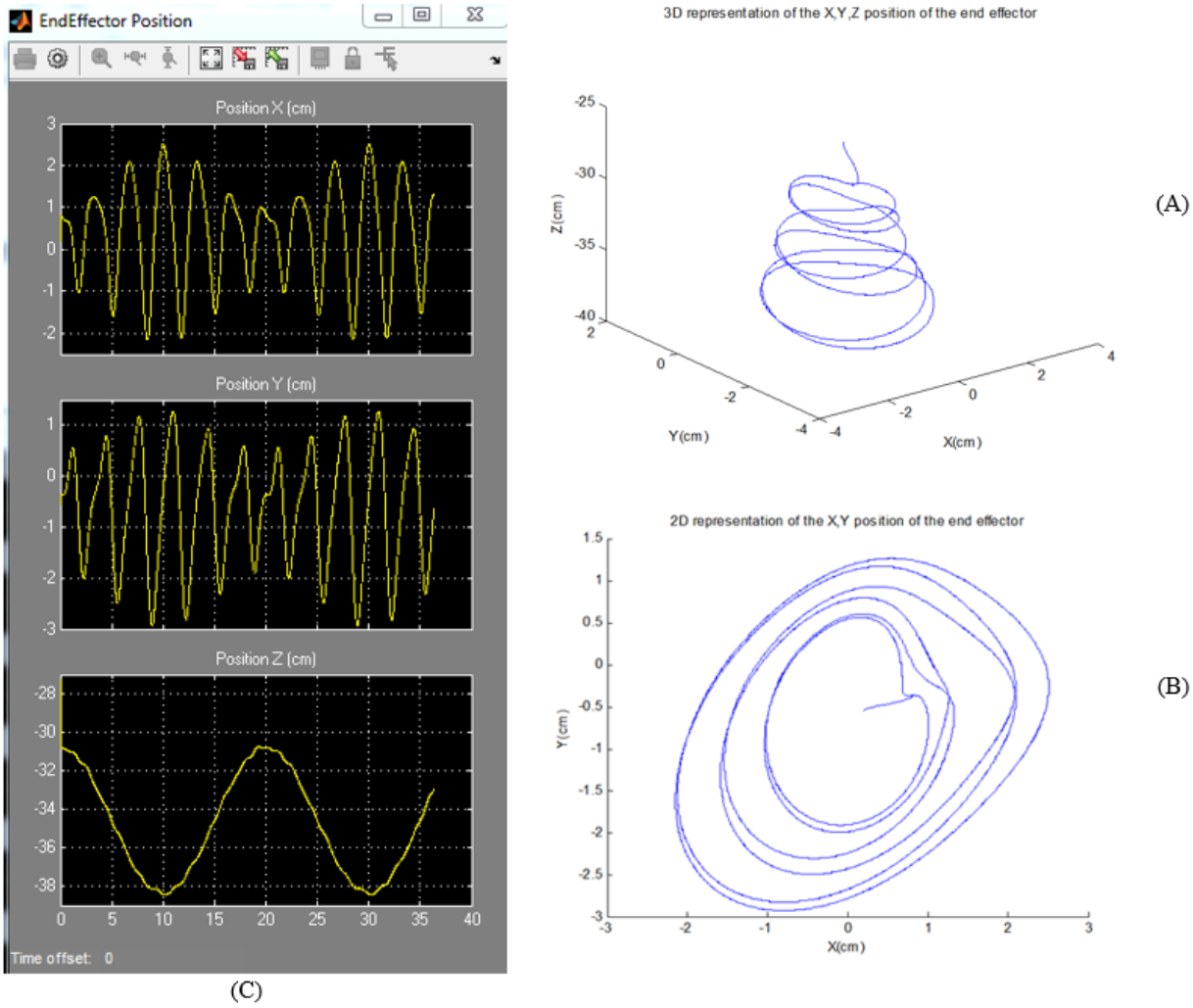

Fig. 18. The platform's end effector position. A plot representing the end effector path in (A) 3D and (B) 2D, (C) the position of the end effector as a function of time as displayed in MATLAB's scope block.

sufficient degree of elasticity to allow the struts to pivot. Testing of the line showed it elongated approx. 1.5mm when supporting a 5kg load. The combined weight of the platform and the Articulated Distal Tip Tool is approximately 8kg. Even allowing for some dynamic loading, the cords are never loaded beyond their breaking stresses, especially as the weight of the platform and tool is distributed between three connection points on each of the upper and lower platforms. The cords did not fail at any time during the testing period. Following the initial assembly of the joints, the tension in the cords was normally adjusted once, via a very simple procedure with a spanner to rotate the threaded tension mechanism after a brief period of use, and then never had to be adjusted again.

The robot platform is validated by modelling and simulation only. The authors are intending to follow up with a study/paper that presents the design of the control scheme and haptic feedback of the robot platform to qualitatively validate the function of the robot experimentally.

9. Conclusion

In this paper, we have developed a robotic platform that could be used in spinal surgery procedures, with promising early results. The surgical robot is a parallel robot platform comprised of multiple struts, arranged in a geometrically stable array, connected at their end points via the CCJ. Each strut, acting as part of a truss, can change in length (telescope), and thus their combined variations can change the overall form of the frame. The CCJ enables multiple struts to be connected and pivot around each node point. The joints have near-perfect concentricity of rotation around the node point, which enables the tension and compression forces of the struts to be resolved in a structurally-efficient manner. The design evolved from an analysis of simple, pure-tension net structures, combined with aspects of rigid space frame structures, to resist compressive forces. The advantages of using such joint connectors were

demonstrated by applying a variable-geometry mount in the design of the surgical robot, to target the removal of cancerous tumours surrounding the spinal column of affected patients. The kinematics were simpler as a direct result of using the concentric joints, which created a form changing platform with the underlying geometry of a pure octahedron, rather than a complex skew hexagonal prism of existing platforms.

In the future, the development of the tele-operation scheme for the robot will be presented, including the design of control and haptic feedback system.

References

[1] M. Diana, J. Marescaux, Robotic surgery, *Brit J Surg*. 102(2) (2015) 15 - 28.

[2] M. Ciftdemir, M. Kaya, E. Selcuk, and E. Yalniz, Tumors of the spine, *World J Orthop*. 7(2) (2016) 109-116.

[3] J. Bodnera, F. Augustina, H. Wykypiela, J. Fisha, G. Muehlmanna, G. Wetscherb, T. Schmida, The da Vinci robotic system for general surgical applications: a critical interim appraisal, *Swiss Medical Weekly*. 19 (135) (2005) 674-678.

[4] C. Detter, H.Reichenspurner, D.H. Boehm and B. Reichart, Robotic manipulators in cardiac surgery: the computer-assisted surgical system ZEUS. *Minimally Invasive Therapy & Allied Technologies*, 10(6) (2001) 275-281.

[5] V. E. Gough, and S. G. Whitehall, *Universal tyre test machine* 1962. *In Proc of the FISITA 9th Int Technical Cong*, (Institution of Mechanical Engineers, 1962) pp. 117-137

[6] D. Stewart, 1965. A Platform with six degree of freedom. *In Proc Instn Mech Engrs* (UK, 1965)180: p. 371-386.

[7] K.L. Cappel, "Motion Simulator", US Patent No. 3,295,224, 3 Jan 1967.

[8] J. U. Duncombe, Infrared navigation—Part I: An assessment of feasibility, *IEEE Trans. Electron Devices*. 11(1) (1967) 34–39.

[9] S. Najarian, and E. Afshari, Evolutions and Future Directions of Surgical Robotics: A Review, *Int. J. Clin. Med*. 3(2) (2012) 75-82.

[10] J.P. Merlet, *Parallel Robots* (Springer, The Netherlands, 2006)

[11] M. Shoham, M. Burman, E. Zehavi, L. Joskowicz, E. Batkilin, and Y. Kunicher, Bone-Mounted Miniature Robot for Surgical Procedures: Concept and Clinical Applications, *IEEE Transactions on Robotics and Automation*. 19(5) (2003) 893 - 901.

[12] H. Tian, D.Wu, Z. Du, J. Ma, L.Sun. Development of a Robot System Assisting Artificial Cervical Disc Replacement Surgery, in *Proc. Int. Conf. Robotics and Biomimetics* (China, Tianjin, 2010), pp. 1382-1387.

[13] A. G. Bell, Tetrahedral Principle in Kite Structure, *National Geographic Magazine*. 14(6) 1903.

[14] T. T. Lan, Space Frame Structures, In *Structural Engineering Handbook* (CRC, Boca Raton, 1999).

[15] P. Harkin, R. Vaidyanathan, S. Morad, Concentric Joint Connectors for Form-Changing Space Frames, in Proc. 7th Int. Conf. Structural Engineering, Mechanics and Computation (Cape Town, South Africa, 2019) pp. 977-982.

[16] P. Bosscher and I. Ebert-Uphoff, A Novel Mechanism for Implementing Multiple Collocated Spherical Joints, in *Proc. Int. Conf. Robotics and Automation* (Taipei, Taiwan, 2003), pp. 336-341.

[17] G. Hamlin, and A. C. Sanderson, A Novel Concentric Multilink Spherical Joint with Parallel Robotics Applications, in *Proc. Int. Conf. Robotics and Automation* (San Diego, CA, USA, 1994), pp. 1267-1272.

[18] P. Harkin, Adjustable Structures, W. PCT, Editor 2014: UK. p. 34.

[19] S. Morad, C. Ulbricht, P. Harkin, J. Chan, K. Parker and R. Vaidyanathan, Modelling and control of a water jet cutting probe for flexible surgical robot. in *Proc. IEEE Int. Conf. Automation Science and Engineering* (Gothenburg, Sweden, 2015), pp. 1159-1164.

[20] Z. Shao, X. Tang, and L. Wang, Optimum Design of 3-3 Stewart Platform Considering Inertia Property. *Advances in Mechanical Engineering*, 2013 (2013) 1-10.

[21] Z. Bingul and O. Karahan, Dynamic Modeling and Simulation of Stewart Platform, in *Serial and Parallel Robot Manipulators - Kinematics, Dynamics, Control and Optimization* (InTech, Rijeka, 2012), pp. 19-42.

Samir Morad received the BEng degree in medical engineering from Queen Mary College, University of London, London, UK, in 2010 and the MSc. degree in biomedical engineering from Imperial College London, London, UK, in 2011, and PhD. degree in medical robotics from Imperial College London, London, UK, in 2015. He is currently a lecturer in mechanical engineering and the leader of the biomedical engineering programme at the department of architecture, computing and engineering at the University of East London.

From 2016 to 2019 Dr Morad was a teaching associate in biomedical engineering at the department of life and health science at Aston University.

From 2015 to 2016 Dr. Morad was a Research Fellow in medical robotics at Bristol Robotics Laboratory. His research interest includes the development of robot assisted flexible surgical intervention, 3D reconstruction and FEA analysis of human tissues.

Christian Ulbricht is a Consultant Spinal Neurosurgeon at Imperial College Healthcare NHS Trust and based at Charing Cross Hospital. He qualified from Medical School in Berlin, Germany but moved to the UK in 1995. He completed his neurosurgical training in London and has been a consultant neurosurgeon since 2006.

Since 2007 Mr. Ulbricht's practice has been exclusively spinal and he has a very wide clinical range from assessing patients with simple back and neck pain to complex spinal surgery.

His interests are spinal surgery for degenerative disease, minimal invasive surgery and surgery for tumors and infections. He is the surgical lead for metastatic spinal cord compression at Imperial College NHS Trust, and he is on the advisory board of the European Spine Journal.

Ravi Vaidyanathan is a Reader in Biomechatronic in the Department of Mechanical Engineering at Imperial College London. He earned his Ph.D. in biologically inspired systems at Case Western Reserve University (USA) in 2001, and worked in industry through 2004, holding two directorships in control systems and medical engineering. Prior to his post at Imperial, he completed a Senior Research Fellowship in Brain-Computer Interface at the University of Southampton, was a Research Assistant Professor of Systems Engineering at the US Naval Postgraduate School, and a Senior Lecturer in Biodynamics at the University of Bristol.
His academic research has translated in a range industrial projects including several new ventures based on principles established in his laboratory

Kim H. Parker received the B.S.E degree in Aeronautical Engineering from Princeton University, USA, in 1962 and the M.A. degree in Aerospace and Mechanical Engineering from Princeton University, USA, in 1964, and PhD degree in Aerospace and Mechanical Engineering from Princeton University, USA, in 1966. He is Emeritus Professor of Physiological Fluid Mechanics at the department of bioengineering, Imperial College London.

Mr. Parker trained at Princeton University as an aeronautical engineer specializing in combustion and rocketry, followed by experience in the Mechanics Department at Johns Hopkins University, but has been studying various aspects of hemodynamics and physiological mechanics since joining the Physiological Flow Studies Unit at Imperial College London over 30 years ago. His work in hemodynamics has included the analysis of the wave nature of flow in the arteries, the hemodynamics of the heart and the coupling of flow from the heart to the arteries, and the experimental and theoretical study of the mechanics of the deep veins of the calf. His work in connective tissue mechanics has included study of the deformation of the red-blood cell membrane, the osmotic pressure in cartilage and the physicochemical properties of elastin.

Paul Harkin received his M.A. degree in Architecture from Birmingham City University, UK in 1997. He became a Chartered Member of the Royal Institute of British Architects in 2002. Since then, he has practiced as an Architect in a variety of Building sectors, notably on Airports and Education Buildings. Since 1992, he has also conducted research into Adaptive Space Frame Structures, and holds several related patents. Paul Harkin is the author and co-author of over 5 technical publications. His research interests focus on Adaptive Structures and their applications in various areas of design and engineering.

Justin Chan received the MEng degree in Mechanical Engineering from Imperial College London, UK, in 2014. He is a senior mechanical engineer at Cytera CellWorks. Mr. Chan is Experienced Design Engineer with a demonstrated history of working in the mechanical, electrical and electronic manufacturing industry focusing on R&D and New Product Innovation. Skilled at concept generation and development from ideation to production. Proficient in programming, design, electronics, prototyping and optimization. He is interested in new innovative, emerging, disruptive technologies.